# $\beta$-Liddle mutation of the epithelial sodium channel increases alveolar fluid clearance and reduces the severity of hydrostatic pulmonary oedema in mice

Nadia Randrianarison[1,2], Brigitte Escoubet[2,3,4], Chrystophe Ferreira[4], Alexandre Fontayne[1,2], Nicole Fowler-Jaeger[5], Christine Clerici[1,2], Edith Hummler[5], Bernard C. Rossier[5] and Carole Planès[1,6]

[1]*INSERM, U773, CRB3, Paris F-75018, France*
[2]*Université Denis Diderot-Paris7, Paris F-75018, France*
[3]*INSERM, U772, Paris F-75005, France*
[4]*CEFI IFR02, Université Denis Diderot-Paris7, Paris F-75018, France*
[5]*Département de Pharmacologie et de Toxicologie, Université de Lausanne, 1005 Lausanne, Switzerland*
[6]*Université de Versailles Saint-Quentin, Versailles F-78000, France*

**Transepithelial sodium transport via alveolar epithelial $Na^+$ channels and $Na^+$,$K^+$-ATPase constitutes the driving force for removal of alveolar oedema fluid. Decreased activity of the amiloride-sensitive epithelial $Na^+$ channel (ENaC) in the apical membrane of alveolar epithelial cells impairs sodium-driven alveolar fluid clearance (AFC) and predisposes to pulmonary oedema. We hypothesized that hyperactivity of ENaC in the distal lung could improve AFC and facilitate the resolution of pulmonary oedema. AFC and lung fluid balance were studied at baseline and under conditions of hydrostatic pulmonary oedema in the $\beta$-Liddle (L) mouse strain harbouring a gain-of-function mutation ($R^{566}{}_{stop}$) within the *Scnn1b* gene. As compared with wild-type (+/+), baseline AFC was increased by 2- and 3-fold in heterozygous (+/L) and homozygous mutated (L/L) mice, respectively, mainly due to increased amiloride-sensitive AFC. The $\beta_2$-agonist terbutaline stimulated AFC in +/+ and +/L mice, but not in L/L mice. Acute volume overload induced by saline infusion (40% of body weight over 2 h) significantly increased extravascular (i.e. interstitial and alveolar) lung water as assessed by the bloodless wet-to-dry lung weight ratio in +/+ and L/L mice, as compared with baseline. However, the increase was significantly larger in +/+ than in L/L groups ($P = 0.01$). Volume overload also increased the volume of the alveolar epithelial lining fluid in +/+ mice, indicating the presence of alveolar oedema, but not in L/L mice. Cardiac function as evaluated by echocardiography was comparable in both groups. These data show that constitutive ENaC activation improved sodium-driven AFC in the mouse lung, and attenuated the severity of hydrostatic pulmonary oedema.**

(Received 26 February 2007; accepted after revision 12 April 2007; first published online 12 April 2007)
**Corresponding author** C. Planès: INSERM 773, CRB3, Faculté de Médecine Xavier Bichat, 16 rue Henri Huchard, BP 416, F-75870 Paris Cedex 18, France. Email: carole.planes@apr.aphp.fr

It is crucial for optimal gas exchange across the air–blood barrier that the pulmonary alveoli remain free of fluid, that is to say that the volume of the alveolar hypophase lining the apical face of alveolar epithelial cells remains as low as possible. The volume of alveolar hypophase is mainly regulated by active vectorial sodium ($Na^+$) transport across the alveolar epithelium (Matthay *et al.* 1982, 2002; Basset *et al.* 1987*a*,*b*). Transcellular $Na^+$ transport is coupled with chloride ion ($Cl^-$) transport in the same direction, and the resulting osmotic gradient locally created provides the driving force for water movement from the alveolus to the pulmonary interstitium. Sodium-driven alveolar fluid clearance (AFC) accounts for the ability of the lung to remove alveolar fluid at the time of birth. It also represents the primary mechanism for removal of oedema fluid from the alveolar space, on condition that the alveolar epithelium remains structurally and functionally intact (Matthay & Wiener-Kronish, 1990). Indeed, it has been shown that patients mechanically ventilated for pulmonary oedema who have maximal AFC (as is mostly the case for hydrostatic pulmonary oedema) have better clinical outcomes than patients with impaired AFC (as is usually the case in the course of acute lung injury; Ware & Matthay, 2001).

There is abundant evidence that the apical amiloride-sensitive epithelial $Na^+$ channel (ENaC)

 DOI: 10.1113/jphysiol.2007.131078

(Canessa *et al.* 1993, 1994) and the basolateral sodium–potassium adenosine triphosphatase ($Na^+$,$K^+$-ATPase) constitute the key components of transcellular alveolar $Na^+$ transport and alveolar fluid balance (Matalon & O'Brodovich, 1999; Matthay *et al.* 2002). The three ENaC subunits $\alpha$, $\beta$ and $\gamma$ as well as $\alpha$- and $\beta$-$Na^+$,$K^+$-ATPase are expressed in both alveolar type I and type II epithelial cells (Planès *et al.* 1997; Johnson *et al.* 2002, 2006; Ridge *et al.* 2003). Importantly, newborn mice with complete inactivation of the *Scnn1a* ($\alpha$-ENaC) gene exhibit abolition of lung $Na^+$ transport and subsequent inability to clear the lungs from fluid at birth (Hummler *et al.* 1996), whereas adult mice with reduced $\alpha$-ENaC expression exhibit decreased AFC and delayed resolution of alveolar oedema (Hummler *et al.* 1997; Egli *et al.* 2004; Li & Folkesson, 2006). In addition, it has been shown that adenovirus-mediated transfer of either $\alpha_2$- or $\beta_1$-$Na^+$,$K^+$-ATPase subunit genes in rat lung *in vivo* increased $Na^+$,$K^+$-ATPase activity in alveolar epithelial cells as well as AFC, and attenuated the severity of acute lung injury (Factor *et al.* 1998, 2000; Azzam *et al.* 2002; Ridge *et al.* 2003). To date, the effect of ENaC hyperactivity in the distal lung, either due to ENaC subunit overexpression or to a gain-of-function mutation, has not been studied.

Here, we hypothesized that an increase in ENaC activity in alveolar epithelial cells could increase AFC, and potentially facilitate the resolution of pulmonary oedema. To address this issue, we studied a previously established knock-in mouse strain carrying a premature Stop codon in the *Scnn1b* ($\beta$-ENaC) gene corresponding to the $R_{566stop}$ gain-of-function mutation found in human patients with Liddle's syndrome (Pradervand *et al.* 1999*a*,*b*). Liddle's syndrome is an autosomal dominant form of salt-sensitive hypertension due to increased $Na^+$ absorption in the distal nephron (Liddle *et al.* 1963). The $R_{566stop}$ mutation leads to the deletion of the $\beta$-ENaC COOH-terminus PY motif, thus abolishing the interaction between ENaC and the ubiquitin protein-ligase Nedd4-2 that targets the channel for endocytosis and degradation (Shimkets *et al.* 1994; Schild *et al.* 1996; Abriel *et al.* 1999). As a result, ENaC activity and $Na^+$ absorption are increased, at least in part, by an increase in channel density at the cell surface (Firsov *et al.* 1996). The $\beta$-Liddle mice reproduce to a large extent the human form of Liddle's disease, with mutated mice displaying constitutive hyperactivity of ENaC in the distal nephron and the distal colon (Pradervand *et al.* 1999*b*, 2003). Their distal lung phenotype, namely alveolar $Na^+$ transport and fluid homeostasis, has not been studied to date.

Therefore, the objectives of the present *in vivo* study were to determine whether the $\beta$-Liddle mutation (L) in mouse would affect (i) $Na^+$-driven AFC under basal and $\beta_2$-agonist-stimulated conditions, and (ii) distal lung fluid homeostasis under conditions of experimental pulmonary oedema. Our data show that the $\beta$-Liddle mutation leads to a marked increase in AFC mostly due to increased ENaC activity, and that it attenuates the severity of experimental hydrostatic pulmonary oedema induced by acute volume overload.

## Methods

### Transgenic mice

The generation of Liddle mice harbouring the $R_{566stop}$ mutation on the *Scnn1b* gene has been previously described (Pradervand *et al.* 1999*a*,*b*). Animals were housed in standard cages and light conditions, and fed standard diet and water *ad libitum*. Heterozygous mutant +/L mice were intercrossed and the resulting offspring were genotyped by PCR on genomic tail DNA at 3 weeks of age, as previously described (Pradervand *et al.* 1999*a*). Experiments were performed on litter-matched mice aged 2–6 months. The investigators were blinded to genotype information for all comparative measurements. The total number of mice used in this study was 180. The experiments were approved by the institutional reviewing board on animal experimentation, and accorded with animal welfare guidelines (Ministère Français de la Pêche et de l'Agriculture, agreement no. 75-1045). At the end of experiments animals were killed with a lethal dose of intraperitoneal pentobarbital (250 mg $kg^{-1}$).

### Lung histology

Lung histology was performed as described by Kaner *et al.* (2000). Animals were killed with intraperitoneal pentobarbital (250 mg $kg^{-1}$), the trachea was cannulated and connected to a syringe before a thoracotomy was performed to remove the lungs. Lungs were inflated to total capacity, placed in 300 ml PBS heated to 60°C for 3 min in a microwave oven, and transferred to 4% paraformaldehyde overnight. The lungs were embedded with paraffin and sections were cut at 4 $\mu$m thickness and stained with haematoxylin and eosin.

### Isolation of mouse bronchiolar–alveolar epithelial cells

Mouse bronchiolar–alveolar epithelial cells (BAEC) were isolated from mice aged 2 months by dispase digestion of lung tissue, followed by sequential filtration and differential adherence on culture dishes coated with rat anti-mouse CD 45 and rat anti-mouse CD 16/32 (BD Pharmingen), as previously described (Corti *et al.* 1996; Planès *et al.* 2005). The yield was $(4–5) \times 10^6$ BAEC per mouse, with a percentage of alveolar type II cells (as assessed by phosphine 3R staining) $\geq$ 78% and a

cell viability > 95%. BAEC were used immediately after isolation for RNA or protein extraction.

### Reverse transcription and real-time RT-PCR analysis

Total RNA was prepared from freshly isolated mouse BAEC using the RNeasy extraction kit (Qiagen, Hilden, Germany). The RNAs (2.5 $\mu$g per sample) were reverse-transcribed at 37°C for 1 h using the Superscript II RNase H reverse-transcriptase (Invitrogen, Basel, Switzerland) and random primers. Two microlitres of the first strand cDNA reaction was amplified using a Roche light cycler and the 2x QuantiTect SYBR Green PCR Master Mix (Qiagen) according to the manufacturer's guidelines. $\beta$-Actin was used as internal control. The sequences of the primers were as follows: mouse $\alpha$-ENaC, sense (S): 5′-CGGAGTTGCTAAACTCAACATC-3′ (position +1638 to +1659; 3′ of the translation start); antisense (AS): 5′-TGGAGACCAGTACCGGCT-3′ (position +1849 to +1866; 3′ of the translation start); mouse $\beta$-ENaC, (S): 5′-ATGTGGTTCCTGCTTACGCTG-3′ (position +151 to +171; 3′ of the translation start); (AS): 5′-GTCCTGGTGGTGTTGCTGTG-3′ (position +397 to +416; 3′ of the translation start); mouse $\gamma$-ENaC, (S): 5′-CCAAAGCCAGCAAATAAACAAA-3′ (position +1479 to +1500; 3′ of the translation start); (AS): 5′-GCGGCGGGCAATAATAGAGA-3′ (position +1691 to +1710; 3′ of the translation start); mouse $\beta$-actin, (S): 5′-CGGAGTTGCTAAACTCAACATC-3′ (position +412 to +432; 3′ of the translation start); (AS): 5′-TGTCACGCACGATTTCCC-3′ (position +697 to +714; 3′ of the translation start). As a negative control, reverse transcription was performed in the absence of enzyme and amplified by PCR.

### Western blot analysis

Freshly isolated mouse BAEC were resuspended in 30 $\mu$l of ice-cold lysis buffer containing 150 mM NaCl, 50 mM Tris-HCl (pH 7.6), 1% Triton X-100, 0.1% SDS, and protease inhibitors, and kept on ice for 1 h. Cell lysates were then centrifuged (12 000 r.p.m. (12880*g*), 15 min) at 4°C, and samples of the supernatants were immediately frozen before use. For Western blotting, samples of protein extracts (30–40 $\mu$g) in one volume of sample buffer (containing 10% glycerol, 12.5% 0.05 M Tris-HCl (pH 6.8), 0.1% SDS, 5% $\beta$-mercaptoethanol, and 0.01% (w/v) bromophenol blue in $H_2O$) were resolved through 10% acrylamide gels, electroblotted, electrically transferred to nitrocellulose paper, and subsequently probed for $\alpha$- or $\gamma$-ENaC subunits. Rabbit polyclonal anti-rat $\alpha$-ENaC and anti-rat $\gamma$-ENaC antibodies (Duc *et al.* 1994) were used at the dilution 1 : 2000, and mouse monoclonal anti-$\beta$-actin at the dilution 1 : 5000. The anti-rabbit IgG secondary antibody (Amersham Pharmacia Biotech, UK) was used at dilution 1 : 5000, and the signal was developed with the ECL+ system (Amersham Pharmacia Biotech, UK). Quantification of ENaC subunit and $\beta$-actin levels was obtained using NIH Image software.

### Measurement of alveolar fluid clearance

Sodium-driven alveolar fluid clearance (AFC) was measured *in vivo* using an *in situ* model of mouse lung as previously described (Fukuda *et al.* 2000; Planès *et al.* 2005). This model has been shown to give AFC values similar to those obtained with the ventilated mouse model over a 15 min period (Fukuda *et al.* 2000). Briefly, male or female wild-type, +/L, or L/L mice aged 2–5 months were killed with intraperitoneal pentobarbital (250 mg kg$^{-1}$) and maintained at 37–38°C using a heating pad, an infrared lamp and an intra-abdominal monitoring thermistor. A 20-gauge venous catheter was inserted in the trachea through a tracheotomy and tightly fixed. The lungs were inflated with 100% $O_2$ at 7 cm$H_2O$ continuous positive airway pressure throughout the experiment. Then, 10 ml kg$^{-1}$ of instillate was delivered to the lungs over 30 s through the tracheal catheter. The instillate consisted of Ringer lactate solution (pH 7.4) adjusted to 325 mosmol (kg $H_2O$)$^{-1}$ with NaCl, containing 5% bovine serum albumin and 0.1 $\mu$Ci ml$^{-1}$ $^{125}$I-albumin (Cis Bio International, Gif-sur-Yvette, France) as a labelled alveolar fluid volume tracer. An alveolar fluid sample (50–100 $\mu$l) was aspirated 1 min after instillation and at the end of experiment (15 min later). The aspirates were centrifuged at 3000 *g* for 10 min, and the radioactivity in supernatants was counted in duplicate. Alveolar fluid clearance (percentage fluid absorption at 15 min) was calculated from the increase in alveolar fluid albumin as follows:

$$\mathrm{AFC} = (C_\mathrm{f} - C_\mathrm{i})/C_\mathrm{f} \times 100,$$

where $C_\mathrm{i}$ and $C_\mathrm{f}$ represent the initial and final concentrations of $^{125}$I-albumin in the aspirate at 1 and 15 min, respectively, as assessed by radioactivity measurements. In some experiments, amiloride (final concentration: 1 mM), terbutaline (final concentration: $10^{-4}$ M) or the cystic fibrosis transmembrane conductance regulator (CFTR) inhibitor glycine hydrazide GlyH-101 (Calbiochem) (final concentration: $5 \times 10^{-5}$ M) were added to the instillate and AFC was measured at 15 min as described above.

### Hydrostatic volume-overload studies

A standard model of acute hydrostatic oedema was used, as previously described (Franck *et al.* 2000; Fang *et al.* 2002). Mice were weighed, anaesthetized with intraperitoneal ketamine (80 mg kg$^{-1}$) and xylazine (12 mg kg$^{-1}$), and

ventilated with a constant volume ventilator (Harvard apparatus) with a tidal volume of 8 ml $kg^{-1}$, a positive end-expiratory pressure of 3 $cmH_2O$ and 100% oxygen. After a 20 min baseline period, a saline infusion via a catheter inserted into the jugular vein was given by an infusion pump over 2 h (total volume = 40% of body weight, with 40% of the total volume given over the first 20 min, the remaining 60% volume given over 100 min). At the end of infusion, the animal was weighed again in order to assess the change in body weight induced by saline infusion and to calculate urinary output over the 2 h period, before being killed by exsanguination and further processed.

### Estimation of pulmonary oedema

Pulmonary oedema was first estimated by calculation of the amount of extravascular lung water (i.e. interstitial + alveolar water), as previously described (Berthiaume *et al.* 1987; Fang *et al.* 2002). Briefly, mice were anaesthetized as described above and killed by exsanguination. A blood sample was obtained for measurement of haemoglobin concentration. Lungs were removed and homogenized for measurement of lung homogenate supernatant haemoglobin concentration, and lung homogenate was placed in an incubator at 80°C for 24 h for dessication. The bloodless wet-to-dry lung weight ratio was calculated using standard methods (Berthiaume *et al.* 1987; Fang *et al.* 2002).

The volume of fluid in the airspace compartment was also estimated from the change in albumin concentration in the alveolar instillate, using a method adapted from Factor *et al.* (2000). Briefly, the volume of alveolar epithelial lining fluid was calculated by instilling 0.3 ml of fluid ($V_0$) containing a known concentration of $^{125}$I-albumin ($C_0$) into the airspace. After 1 min mixing in the lungs inflated at 7 $cmH_2O$ continuous positive airway pressure, the instillate was aspirated and the concentration of $^{125}$I-albumin ($C_1$) was measured. The volume of alveolar epithelial lining fluid ($V_{ELF}$) was calculated as follows:

$$V_{ELF} = V_0(C_0/C_1) - V_0.$$

### Echocardiographic analysis

Echocardiography was performed on lightly anaesthetized adult mice (isoflurane (Abbot Laboratories Ltd) in oxygen) (4- to 5-months-old; body weight, 22–35 g) with a Toshiba Power Vision 6000 (SSA 370A) equipped with a linear 8–14 MHz transducer, as previously described (Parlakian *et al.* 2005). Data were transferred online to a computer for offline analysis (Ultrasound Image Workstation-300A, Toshiba). The left ventricle (LV) was imaged in parasternal long-axis view to obtain measurements of left atrium and LV in time-motion mode. Ejection fraction (EF) was calculated as follows: $EF = (LVEDD^3 - LVESD^3)/LVEDD^3$, where LVEDD is the (LV end-diastolic diameter and LVESD is the LV end-systolic diameter. The mean velocity of circumferential fibre shortening (Vcfc) was corrected for heart rate and calculated as follows: Vcfc = SF/ETc, where SF is shortening fraction obtained as SF = (LVEDD − LVESD)/LVEDD, and ETc is the ejection time corrected for heart rate (as ET divided by square root of R–R interval). Pulsed-wave Doppler tissue images were obtained from the posterior wall for the measurement of maximal systolic wall velocities. The apical view was used for pulsed-wave Doppler measurements of LV mitral flow (E wave) and LV aortic outflow, and time–motion colour Doppler mode (E wave propagation velocity (E)) and for tissue Doppler measurement of mitral annulus velocities (systolic wave Sa, and diastolic wave Ea). E/Ea was computed as an estimate of LV filling pressure.

### Statistical analysis

Results are presented as means ± S.E.M. For functional data, one-way variance analyses were performed and, when allowed by the $F$ value, results were compared by the modified least significant difference (Statview software, Abacus Concepts, Berkeley, CA, USA). For Western blot experiments, differences between groups were evaluated with an unpaired $t$ test performed on raw densitometric data. $P < 0.05$ was considered significant.

## Results

### Lung histology

Lung macroscopic appearance was similar in wild-type (WT) and $\beta$-ENaC L/L mice. Histological examination of the lungs revealed no morphological difference between the two groups (Fig. 1). In particular, the histological aspects of the distal lung including bronchioles, alveolar ducts, alveolar epithelium and blood vessels appeared normal in $\beta$-ENaC L/L mice.

### Expression of ENaC subunits in bronchiolar–alveolar cells

To determine whether the $R_{566stop}$ Liddle mutation on the *Scnn1b* gene encoding the $\beta$-ENaC subunit modified the expression of either $\alpha$-, $\beta$- or $\gamma$-ENaC mRNA transcripts in the distal lung, real-time RT-PCR experiments were performed on BAEC freshly isolated from littermate +/+ and $\beta$-ENaC L/L mice. The levels of $\alpha$-ENaC and $\gamma$-ENaC mRNA transcripts (relative to $\beta$-actin mRNA) expressed

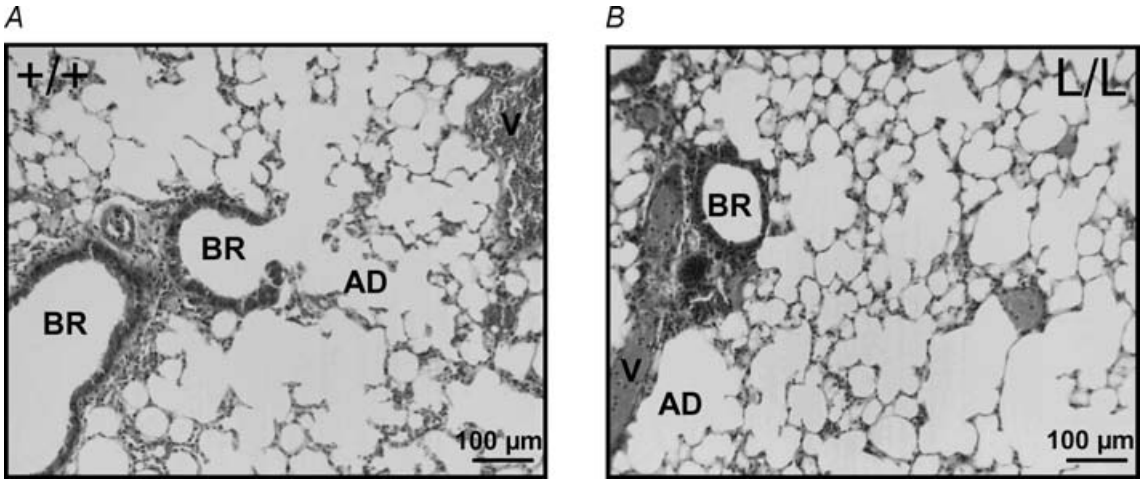


**Figure 1. Photomicrographs of the distal lung in wild-type and Liddle mice**
Photomicrographs of representative lung sections of wild-type (+/+; *A*) and homozygous mutated (L/L; *B*) littermates. The morphological aspects of blood vessels (V), bronchioles (BR), alveolar ducts (AD) and alveoli were normal in L/L mice.

in BAEC were not significantly different in $\beta$-ENaC L/L and WT mice (Fig. 2). The expression of $\beta$-ENaC mRNA was reduced by 52% in BAEC from L/L mice as compared with WT ($P = 0.05$), in accordance with what was previously observed in the colon and kidney from these mice (Pradervand *et al.* 1999*b*) (Fig. 2).

Protein expression of $\alpha$- and $\gamma$-ENaC subunits was also evaluated in BAEC extracts by Western blotting. As shown in Fig. 3*A*, immunoblotting with anti-$\alpha$-ENaC revealed a single band migrating at 85 kDa, whereas immunoblotting with anti-$\gamma$-ENaC revealed a major band migrating at 75 kDa and a minor band around 90 kDa, as previously reported (Hughey *et al.* 2004). Quantitative analysis showed that the expression of $\alpha$-ENaC and $\gamma$-ENaC proteins (relative to $\beta$-actin) was not modified in BAEC from $\beta$-ENaC L/L mice as compared with +/+ mice (Fig. 3*B*).

## Alveolar fluid clearance under basal- and $\beta_2$-agonist-stimulated conditions

Sodium-driven alveolar fluid clearance (AFC) was assessed in wild-type (+/+), $\beta$-ENaC +/L and $\beta$-ENaC L/L mice using an *in situ* non-ventilated mouse lung model (Fig. 4). Basal AFC was significantly increased by almost twofold in +/L mice and by almost threefold in L/L mice, as compared with +/+ mice. Amiloride in the alveolar instillate decreased AFC by 65–70% in the three groups. The amiloride-sensitive component of AFC (calculated as the difference between mean basal AFC value and mean AFC value in the presence of amiloride) was $6.2 \pm 0.77\%$ of fluid cleared $(15\,\text{min})^{-1}$ in +/+ mice, $10.5 \pm 0.68\%$ in +/L mice ($P < 0.05$, as compared with WT) and $17.1 \pm 1.42\%$ in L/L ($P < 0.001$, as compared with WT), indicating a good genotype–phenotype relationship. The amiloride-insensitive component of AFC was significantly increased in L/L mice compared to +/+ mice.

AFC was also measured under $\beta_2$-agonist-stimulated condition (Fig. 4). Terbutaline in the alveolar instillate significantly and markedly increased AFC by 73% in +/+

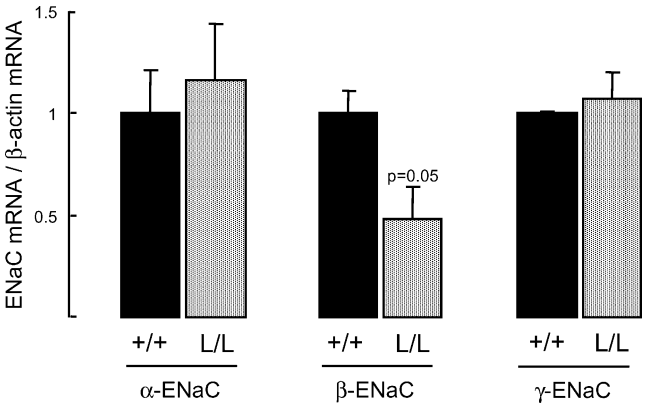


**Figure 2. Expression of ENaC mRNA transcripts in bronchiolar–alveolar epithelial cells from wild-type and Liddle mice**
Bronchiolar–alveolar epithelial cells were isolated from wild-type (+/+) and homozygous mutated (L/L) littermates. Total RNA was extracted from freshly isolated cells, and reverse transcribed. Each sample was amplified by real-time RT-PCR with sets of primers specific for $\alpha$-mENaC, $\beta$-mENaC, $\gamma$-mENaC and $\beta$-actin, as described in Methods. Data were normalized for the corresponding $\beta$-actin signal in each sample. Results are expressed as the ratio of $\alpha$-, $\beta$- or $\gamma$-mENaC mRNA/$\beta$-actin mRNA, and represent means ± S.E.M. (4–5 mice per group). Black bars: wild-type (+/+) group; grey bars: homozygous mutated (L/L) group.

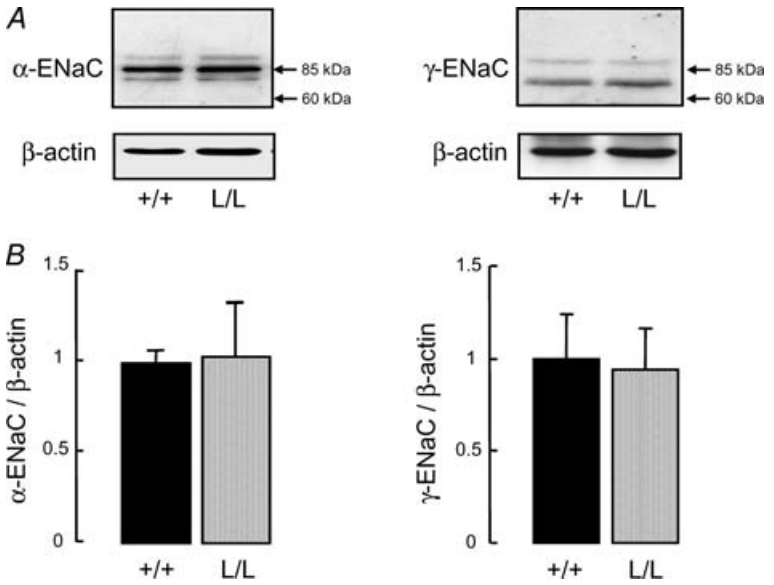


**Figure 3. Expression of $\alpha$- and $\gamma$-ENaC subunit proteins in bronchiolar–alveolar epithelial cells from wild-type and Liddle mice**
Bronchiolar–alveolar epithelial cells (BAEC) were isolated from wild-type (+/+) and homozygous mutated (L/L) littermates. Western blotting was performed on whole-cell extracts as described in Methods. *A*, representative immunoblots showing the expression of $\alpha$-ENaC subunit (left panel), $\gamma$-ENaC subunit (right panel), and of the intracellular protein $\beta$-actin. *B*, quantification of $\alpha$-ENaC (left panel) and $\gamma$-ENaC (right panel) signals in BAEC from +/+ (black bars) and L/L (grey bars) mice was obtained using NIH Image software, and data were normalized for the corresponding $\beta$-actin signal. Results are expressed as the ratio of $\alpha$- or $\gamma$-ENaC/$\beta$-actin, and represent means ± S.E.M. (3–4 animals per group). There was no significant difference between the two groups.

mice. It also moderately but significantly increased AFC by 25% in +/L mice, but was without effect in L/L mice. Despite the lack of stimulation, AFC measured in the presence of terbutaline was still significantly higher in L/L mice than in +/+ mice.

## Effect of CFTR inhibition on alveolar fluid clearance

Recent studies suggested that chloride ($Cl^-$) absorption through CFTR was essential for alveolar fluid clearance, at least under conditions of cAMP stimulation (Jiang *et al.* 1998, 2001; Fang *et al.* 2002). To determine whether or not

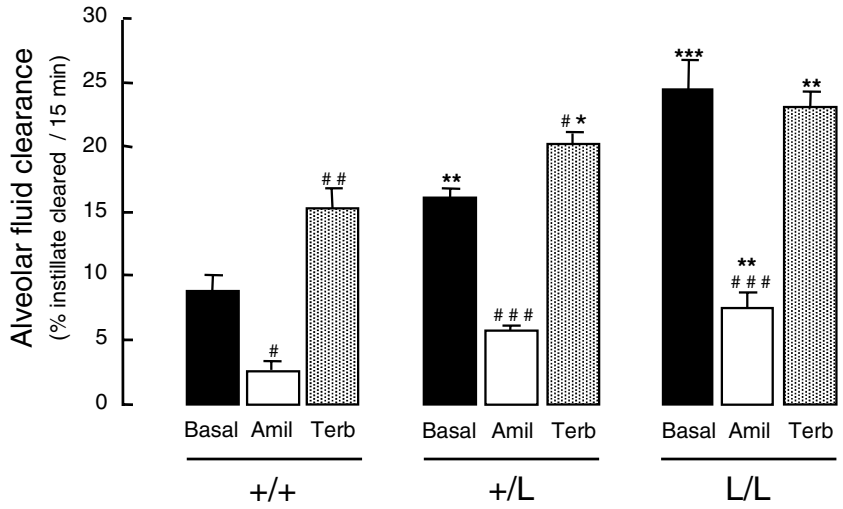


**Figure 4. Alveolar fluid clearance under basal and $\beta_2$-agonist-stimulated conditions in wild-type and Liddle mice**
Sodium-driven alveolar fluid clearance was measured at baseline (Basal, black bars) over a 15 min period in wild-type (+/+), heterozygous (+/L) and homozygous mutated (L/L) littermates aged 2–5 months at 37°C using an *in situ* non-ventilated model in which the airspace was instilled with an isosmolar Ringer lactate solution containing $^{125}$I-albumin as a volume marker, as described in Methods. When indicated, amiloride (final concentration: $10^{-3}$ M) (Amil, open bars), or terbutaline (final concentration:$10^{-4}$ M) (Terb, grey bars) were added to the instillate. Results are expressed as percentage fluid absorption at 15 min, and represent means ± S.E.M. of 4–9 mice per condition. *, **, ***: significantly different from wild-type (+/+) group ($P < 0.05$, $P < 0.01$ and $P < 0.001$, respectively); #, ##, ###: significantly different from corresponding basal value ($P < 0.05$, $P < 0.01$ and $P < 0.001$, respectively).

the ENaC-dependent increase in AFC observed in L/L mice independently of $\beta_2$-receptor stimulation was associated with increased activity of CFTR, AFC was measured in +/+ and L/L littermate mice in the presence or absence of the CFTR inhibitor glycine hydrazide (GlyH-101, final concentration in the alveolar instillate: $5 \times 10^{-5}$ M) (Muanprasat *et al.* 2004). Treatment with GlyH-101 had no significant effect on AFC in either +/+ mice ($8.35 \pm 2.15$ *versus* $7.1 \pm 1.05\%$ fluid cleared $(15\ \text{min})^{-1}$ in treated and untreated groups, respectively; $n = 4$–6 per group; not significant (n.s.)), or L/L mice ($18.7 \pm 3.44$ *versus* $16 \pm 0.97\%$ fluid cleared $(15\ \text{min})^{-1}$ in treated and untreated groups, respectively; $n = 4$–5 per group; n.s.), suggesting that the increase in ENaC-mediated alveolar $Na^+$ transport in L/L mice was not accompanied by an increase in CFTR-mediated chloride absorption.

### Hydrostatic volume-overload model of pulmonary oedema

In order to determine whether the increase in AFC observed in $\beta$-ENaC L/L mice could modulate the severity of hydrostatic pulmonary oedema, ventilated +/+ and L/L mice were submitted to acute intravascular volume expansion by saline infusion (40% body weight within 2 h), and pulmonary oedema was quantified. Comparison of body weight before and at the end of the 2 h saline infusion revealed that the net increase in body weight was $28.9 \pm 2.16\%$ and $31.2 \pm 2.15\%$ in WT and L/L mice, respectively (n.s.), and that urinary output during the 2 h period represented $31.9 \pm 4.14\%$ and $22 \pm 5.49\%$ of the volume infused in WT and L/L mice, respectively ($P = 0.09$). In WT mice, the amount of extravascular lung water as assessed by the bloodless lung wet-to-dry weight ratio increased by 42% following saline infusion as compared with baseline (Fig. 5*A*). Saline infusion also significantly increased the bloodless lung wet-to-dry weight ratio in L/L mice, but this increase was of lesser magnitude than in WT mice ($+0.72 \pm 0.13$ *versus* $+1.58 \pm 0.20\ \text{g g}^{-1}$ in L/L and +/+ groups, respectively; $P < 0.01$). Indeed, the bloodless lung wet-to-dry weight ratio after saline infusion was significantly lower in L/L mice than in WT mice (Fig. 5*A*). The volume of the alveolar epithelial lining fluid (ELF) was next calculated using a method based on the concentration/dilution of instilled $^{125}$I-albumin. As seen in Fig. 5*B*, the volume of ELF was near zero or even slightly negative in WT and L/L mice under basal conditions as well as in L/L mice exposed to volume overload. The slightly negative values of calculated ELF in these conditions reflect the concentration of instilled $^{125}$I-albumin over the 1 min period that is left in the alveolar space because of net alveolar fluid reabsorption. By contrast, in WT mice exposed to volume overload, instilled $^{125}$I-albumin was diluted and the volume of ELF was significantly and markedly increased, reflecting the presence of alveolar oedema fluid.

### Cardiac function

Because the severity of hydrostatic volume-overload pulmonary oedema could be affected by difference in cardiac function between littermate WT and L/L mice, heart function was assessed with non-invasive transthoracic Doppler echocardiography (Table 1). The heart weight to body weight ratio was similar in both groups ($4.63 \pm 0.21$ *versus* $4.60 \pm 0.26\ \text{mg g}^{-1}$ in +/+ and L/L groups, respectively; n.s.; $n = 5$–7 mice per group). Mutant L/L mice LV was neither dilated (as depicted by LVEDD) nor hypertrophied (as depicted by LV mass index). Echocardiographic parameters of contractility (EF, mean shortening velocity of circumferential fibres corrected for heart rate, systolic mitral annulus

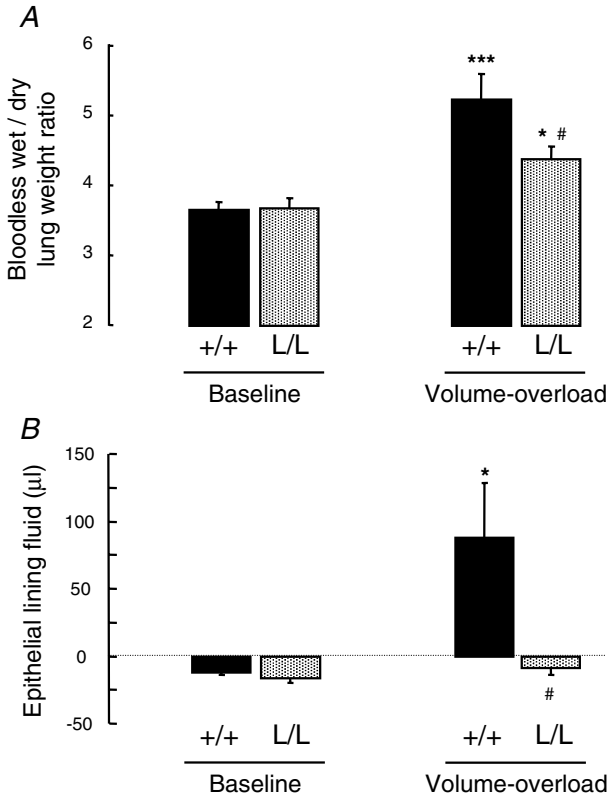


**Figure 5. Effect of acute volume overload on lung fluid balance in wild-type and Liddle mice**
The bloodless lung wet-to-dry weight ratio (*A*) reflecting extravascular lung water, and the volume of the alveolar epithelial lining fluid (*B*) were measured at baseline and at the end of acute saline infusion (40% body weight over 2 h, see Methods) in wild-type (+/+) (black bars) and L/L mice (grey bars). Results represent means ± S.E.M. of 6–9 mice per condition. *, ***: significantly different from corresponding baseline ($P < 0.05$ and $P < 0.001$, respectively); #: significantly different from the wild-type group ($P < 0.05$).

**Table 1. Cardiac evaluation by Doppler echocardiography in wild-type and L/L littermates**

| | +/+ ($n = 5$) | L/L ($n = 7$) | *P* |
|---|---|---|---|
| Body weight (g) | $28.8 \pm 2.20$ | $27.1 \pm 1.94$ | 0.57 |
| Heart rate (beats $min^{-1}$) | $553 \pm 16$ | $544 \pm 16$ | 0.68 |
| LVMI (mg $g^{-1}$) | $4.16 \pm 0.27$ | $3.85 \pm 0.27$ | 0.51 |
| LVEDD (mm) | $3.84 \pm 0.08$ | $3.95 \pm 0.13$ | 0.50 |
| EF (%) | $87 \pm 2$ | $85 \pm 1$ | 0.41 |
| Vcfc (circ $s^{-1}$) | $3.38 \pm 0.20$ | $3.11 \pm 0.12$ | 0.39 |
| Sa (cm $s^{-1}$) | $3.09 \pm 0.23$ | $2.93 \pm 0.33$ | 0.70 |
| IVRT (ms) | $15.6 \pm 0.33$ | $15.1 \pm 1.05$ | 0.68 |
| Ea (cm $s^{-1}$) | $4.71 \pm 0.38$ | $5.11 \pm 0.36$ | 0.47 |
| E/Ea | $21.6 \pm 1.94$ | $16.3 \pm 0.36$ | 0.33 |

LVMI indicates left ventricle (LV) mass index (mg LV (g body weight)$^{-1}$); LVEDD, left ventricle end-diastolic diameter; EF, ejection fraction; Vcfc, velocity of circumferential fibre shortening corrected for heart rate (circ, circumference); Sa, systolic mitral annulus maximal velocity; IVRT, isovolumic relaxation time; Ea, diastolic mitral annulus maximal velocity; E, E wave propagation velocity; and E/Ea, blood to mitral annulus diastolic velocity ratio. No significant difference was found between the two groups.

maximal velocity) and relaxation (isovolumic relaxation time, diastolic mitral annulus maximal velocity) were similar in +/+ and L/L mice (Table 1).

## Discussion

The present study was designed to evaluate *in vivo* the effect of the gain-of-function $R_{566stop}$ Liddle mutation affecting *Scnn1b* ($\beta$-ENaC) gene on mouse $Na^+$-driven AFC and lung fluid homeostasis. We show that under basal conditions AFC was markedly increased in $\beta$-ENaC +/L and $\beta$-ENaC L/L mice compared to WT (+/+) mice, revealing a good genotype–phenotype relationship. This increase in AFC was mostly due to an increase in the amiloride-sensitive part of the clearance, reflecting ENaC activation in Liddle mice. Alveolar treatment with the $\beta_2$-agonist terbutaline significantly increased AFC in WT mice, but was less effective in +/L mice and completely ineffective in L/L mice, indicating a loss of response to $\beta_2$-agonists. Finally, when submitted to acute volume overload, $\beta$-ENaC L/L developed less pulmonary oedema than WT mice, although the cardiac function at baseline was similar in both groups. Our data provide the first evidence that constitutive hyperactivity of ENaC in the distal lung as encountered in $\beta$-ENaC Liddle mice strongly stimulates AFC, and attenuates the severity of hydrostatic pulmonary oedema.

Active transcellular $Na^+$ transport by alveolar epithelial cells is a driving force for the reabsorption of fluid from the alveolar space, and represents the main mechanism for the resolution of alveolar oedema (see for review Matthay *et al.* 2002). The apical amiloride-sensitive ENaC is usually considered as the rate-limiting step in alveolar $Na^+$ transport since newborn mice harbouring complete invalidation of *Scnn1a* ($\alpha$-ENaC) gene die from failure to clear their lungs of fluid at birth (Hummler *et al.* 1996) and adult mice with decreased *Scnn1a* gene expression in the lung show reduced AFC and delayed resolution of alveolar oedema (Hummler *et al.* 1997; Egli *et al.* 2004; Li & Folkesson, 2006). Unlike work on $Na^+$,$K^+$-ATPase (Factor *et al.* 1998, 2000; Azzam *et al.* 2002; Ridge *et al.* 2003), no model of ENaC hyperactivity or overexpression in the alveolar epithelium has been studied to date. We reasoned that if ENaC is truly rate-limiting for alveolar $Na^+$ transport, then ENaC hyperactivity in alveolar epithelial cells should increase AFC, and possibly decrease the severity of alveolar oedema by hastening its resolution. In the present study, we used the $\beta$-Liddle knock-in mouse strain (Pradervand *et al.* 1999*a*,*b*) to test this hypothesis. Because the lung phenotype of these mice had not been previously characterized, we first performed a histological examination of the distal lung and found no morphological difference between WT and $\beta$-ENaC L/L mice. Moreover, molecular studies revealed that mRNA transcript and protein expression levels of $\alpha$- and $\gamma$-ENaC subunits were comparable in BAEC isolated from WT and $\beta$-ENaC L/L. This latter finding, consistent with a previous report involving primary cultures of cortical collecting duct cells from $\beta$-ENaC Liddle mice (Pradervand *et al.* 2003), indicates that the $R_{566stop}$ mutation affecting the $\beta$-ENaC gene did not modify the expression of other ENaC subunits. By contrast, $\beta$-ENaC mRNA transcripts were reduced by one half in L/L mouse BAEC. This decrease in $\beta$-ENaC expression, also evidenced in the colon and kidney from L/L mice (Pradervand *et al.* 1999*b*), could be due to $\beta$-ENaC mRNA instability. Unfortunately, we were not able to quantify the expression of the mutated $\beta$-ENaC protein in BAEC, inasmuch as the antibodies currently used to detect the $\beta$-ENaC subunit recognize the COOH-terminus of the protein which is deleted in the $R_{566stop}$ mutation.

Functional *in vivo* experiments performed under basal conditions showed an almost threefold increase in total AFC in $\beta$-ENaC L/L as compared with +/+ mice, with an intermediate phenotype for $\beta$-ENaC +/L mice. This increase was mostly related to an increase in ENaC-mediated $Na^+$ transport, inasmuch as the amiloride-sensitive part of the clearance represented $6.2 \pm 0.77\%$, $10.5 \pm 0.68\%$ and $17.1 \pm 1.42\%$ in +/+, +/L and L/L mice, respectively. Such an increase in ENaC-mediated $Na^+$ absorption has been previously reported *in vivo* or *in vitro* in various organs from Liddle mice, including the renal cortical collecting duct (Pradervand *et al.* 2003; Chang *et al.* 2005), the distal colon (Pradervand *et al.* 1999*b*) and more recently the trachea (Mall *et al.* 2006), indicating that the Liddle

mutation has functional consequences in most (if not all) $Na^+$-transporting epithelia. Our data provide clear *in vivo* evidence that constitutive activation of ENaC in the distal lung is responsible for increased water reabsorption from the alveolar space, and confirm the prominent role of ENaC in transepithelial alveolar $Na^+$ and fluid transport. Our experiments also evidenced an increase in the amiloride-insensitive component of AFC in L/L mice, in accordance with previous *in vitro* observations that the amiloride-insensitive component of transepithelial transport was increased in primary cultures of renal cortical collecting duct cells from heterozygous and homozygous mutated $\beta$-Liddle mice (Pradervand *et al.* 2003; Chang *et al.* 2005). This could be due to either a change in ENaC sensitivity to amiloride block, or to the activation of ion transport systems distinct from ENaC. This question was not addressed in the present study, but it was previously shown in the *Xenopus laevis* oocyte expression system that the dissociation constant ($K_d$) for amiloride was not modified in the $R_{564stop}$ $\beta$-Liddle rat ENaC mutant as compared with WT (Schild *et al.* 1995).

Next, we tested the effect of the $\beta_2$-agonist terbutaline on AFC in the Liddle mouse strain. Stimulation of $\beta_2$-adrenergic receptors, either by endogenous catecholamines or by $\beta_2$-agonist drugs, induces a marked increase in alveolar $Na^+$ transport and fluid clearance *in vivo* in most mammalian species (Berthiaume *et al.* 1987; Matthay *et al.* 2002). *In vitro*, cAMP agonists have been shown to augment ENaC activity and transepithelial $Na^+$ transport in various cell types including native alveolar epithelial cells, mostly by increasing the turnover and promoting the delivery of ENaC subunits to the cell surface (Snyder, 2000; Jain *et al.* 2001; Planès *et al.* 2002). Here, we found that the stimulatory effect of terbutaline on AFC was clearly present in $\beta$-ENaC +/+ mice, but attenuated in $\beta$-ENaC +/L mice and completely abolished in $\beta$-ENaC L/L mice. The lack of effect of terbutaline on Liddle mice AFC is consistent with a previous report showing that the $R_{566stop}$ mutation of the $\beta$-ENaC gene completely abolished *in vitro* the cAMP-mediated stimulation of $Na^+$ current in the Fischer rat thyroid epithelial cell expression system (Snyder, 2000). Several mechanisms could be involved in this phenomenon. One explanation would be that because the deletion of the PY-motif in $\beta$-ENaC COOH-terminus disrupts ENaC endocytosis and increases the channel cell surface expression, intracellular pools of ENaC might be depleted and therefore exocytosis in response to cAMP might be limited. Another explanation would be that the PY-motif itself might function as a signal for ENaC exocytosis, or might be involved in the retention of ENaC in intracellular pools. Finally, it is also possible that AFC in $\beta$-Liddle mice is already maximal under basal conditions and that nothing could increase it further. It should be noted that AFC in L/L mice, although not responsive to terbutaline, was significantly higher than AFC in terbutaline-treated WT mice. This suggests that under pathological conditions when $\beta_2$-adrenergic receptors are stimulated by endogenous catecholamines (Pittet *et al.* 1994; Fang *et al.* 2002), Liddle mice still have a potentially greater ability to remove fluid from their lungs than WT mice.

There is increasing evidence suggesting that $Cl^-$ absorption through CFTR plays an essential role in AFC, at least in cAMP-mediated up-regulated fluid transport (Jiang *et al.* 1998, 2001; Fang *et al.* 2002). The $\beta$-Liddle mice in which ENaC is constitutively activated independently of cAMP stimulation represent an interesting model for studying the functional link between ENaC and CFTR in the distal lung. To determine whether or not the increase in alveolar $Na^+$ transport in Liddle mice was associated with an activation of CFTR-mediated $Cl^-$ absorption, we tested the effect of the luminally active CFTR inhibitor glycine hydrazide (GlyH-101; Muanprasat *et al.* 2004) on AFC. In WT mice, GlyH-101 failed to inhibit AFC, a finding which is consistent with previous work showing that basal AFC was not modified in cystic fibrosis $\Delta$F508 mice as compared with WT, and that glibenclamide in the alveolar instillate was without effect on WT mice AFC (Fang *et al.* 2002). Of note, GlyH-101 also failed to inhibit AFC in L/L mice. This strongly suggests that under baseline conditions there is no functional activation of CFTR in this model of ENaC hyperactivity.

To test whether the functional differences observed could be relevant in pathological conditions, mice were exposed to an established model of acute hydrostatic pulmonary oedema (Fang *et al.* 2002). Hydrostatic stress with volume overload resulted in significantly more pulmonary oedema in WT mice than in $\beta$-ENaC L/L mice, as assessed by the lung wet-to-dry weight ratio reflecting the amount of extravascular lung water. Indeed, saline infusion did increase the volume of the epithelial lining fluid in WT mice but not in L/L mice, indicating the presence of alveolar oedema only in WT mice. We used an experimental model of hydrostatic pulmonary oedema because this model is presumably less prone to inducing alveolar epithelial cell damage than other experimental models of acute lung injury (Ware & Matthay, 2001). Moreover, it has been previously shown that most patients with hydrostatic pulmonary oedema have preserved alveolar fluid clearance, whereas the majority of patients with acute lung injury or respiratory distress syndrome have impaired alveolar fluid clearance (Matthay *et al.* 1990; Verghese *et al.* 1999; Ware & Matthay, 2001). As expected, histological examination of the distal lung following saline infusion revealed no gross alteration of the alveolar epithelial structure (not shown). The severity of pulmonary oedema induced by acute volume expansion is likely to be affected by the haemodynamic status, i.e. by cardiac and renal function. Here, we found that

echocardiographic parameters at baseline were similar in WT and $\beta$-ENaC L/L mice. This is not surprising since it has been shown that L/L mice fed with a normal salt diet, although they exhibit very low plasma aldosterone levels suggesting salt retention and hypervolaemia, do not develop systemic hypertension that could lead to LV hypertrophy and cardiac dysfunction (Pradervand *et al.* 1999*b*). With regard to the renal function, we found that urinary output during the saline infusion period tended to be lower in L/L mice compared with WT mice, most likely because of constitutive increased ENaC activity in the distal nephron (Pradervand *et al.* 1999*b*, 2003; Chang *et al.* 2005), but the difference was not significant ($P = 0.09$). Therefore, it appears that the reduced severity of pulmonary oedema in L/L mice could probably not be explained by changes in either cardiac or renal function. This strongly supports the concept that increased alveolar $Na^+$ transport due to ENaC activation can reduce alveolar oedema accumulation by favouring oedema fluid removal.

In conclusion, this study highlights the crucial role of ENaC in transepithelial alveolar $Na^+$ transport and alveolar fluid balance in the mouse. Indeed, our finding that ENaC hyperactivity in the distal lung results *in vivo* in increased AFC and reduced severity of pulmonary oedema following acute volume overload suggests that new therapies targeted at enhancing ENaC activity and AFC could hasten the resolution of hydrostatic pulmonary oedema in patients.

## References


Abriel H, Loffing J, Rebhun JF, Pratt JH, Schild L, Horisberger J-D, Rotin D & Staub O (1999). Defective regulation of the epithelial sodium channel by Nedd4 in Liddles's syndrome. *J Clin Invest* **103**, 667–673.

Azzam ZS, Dumasius V, Saldias FJ, Adir Y, Sznajder JI & Factor P (2002). Na,K-ATPase overexpression improves alveolar fluid clearance in a rat model of elevated left atrial pressure. *Circulation* **105**, 497–501.

Basset G, Crone C & Saumon G (1987*a*). Significance of active ion transport in transalveolar water absorption: a study on isolated rat lung. *J Physiol* **384**, 311–324.

Basset G, Crone C & Saumon G (1987*b*). Fluid absorption by rat lung *in situ*: pathways for sodium entry in the luminal membrane of alveolar epithelium. *J Physiol* **384**, 325–345.

Berthiaume Y, Staub NC & Matthay MA (1987). $\beta$-Adrenergic agonists increase lung liquid clearance in anesthetized sheep. *J Clin Invest* **79**, 335–343.

Canessa CM, Horisberger JD & Rossier BC (1993). Epithelial sodium channel related to proteins involved in neurodegeneration. *Nature* **361**, 467–470.

Canessa CM, Schild L, Buell G, Thorens B, Gautschi I, Horisberger J-D & Rossier BC (1994). Amiloride-sensitive epithelial $Na^+$ channel is made of three homologous subunits. *Nature* **367**, 463–467.

Chang C-T, Bens M, Hummler E, Boulkroun S, Schild L, Teulon J, Rossier BC & Vandewalle A (2005). Vasopressin-stimulated CFTR $Cl^-$ currents are increased in the renal collecting duct cells of a mouse model of Liddle's syndrome. *J Physiol* **562**, 271–284.

Corti M, Brody AR & Harrison JH (1996). Isolation and primary culture of murine alveolar type II cells. *Am J Respir Cell Mol Biol* **14**, 309–315.

Duc C, Farman N, Canessa CM, Bonvalet J-P & Rossier BC (1994). Cell-specific expression of epithelial sodium channel $\alpha$, $\beta$ and $\gamma$ subunits in aldosterone-responsive epithelia from the rat: localization by in situ hybridization and immunocytochemistry. *J Cell Biol* **127**, 1907–1921.

Egli M, Duplain H, Lepori M, Cook S, Nicod P, Hummler E, Sartori C & Scherrer U (2004). Defective respiratory amiloride-sensitive sodium transport predisposes to pulmonary oedema and delays its resolution in mice. *J Physiol* **560**, 857–865.

Factor P, Dumasius V, Saldias F, Brown LA & Sznajder JI (2000). Adenovirus-mediated transfer of an Na,K-ATPase $\beta_1$ subunit gene improves alveolar fluid clearance and survival in hyperoxic lung injury. *Hum Gene Ther* **11**, 2231–2242.

Factor P, Saldias F, Ridge K, Dumasius V, Zavner J, Jaffe HA, Blanco G, Barnard M, Mercer R, Perrin R & Sznajder JI (1998). Augmentation of lung liquid clearance via adenovirus-mediated transfer of a Na,K-ATPase $\beta_1$ subunit gene. *J Clin Invest* **102**, 1421–1430.

Fang X, Fukuda N, Barbry P, Sartori C, Verkmann AS & Matthay MA (2002). Novel role for CFTR in fluid absorption from distal airspaces of the lung. *J Gen Physiol* **119**, 199–207.

Firsov D, Schild L, Gautschi I, Mérillat A-M, Schneeberger E & Rossier BC (1996). Cell surface expression of the epithelial Na channel and a mutant causing Liddle syndrome: a quantitative approach. *Proc Natl Acad Sci U S A* **93**, 15370–15375.

Franck JA, Wang Y, Oscar O & Matthay MA (2000). $\beta$-Adrenergic agonist therapy accelerates the resolution of hydrostatic pulmonary oedema in sheep and rats. *J Appl Physiol* **89**, 1255–1265.

Fukuda N, Folkesson HG & Matthay MA (2000). Relationship of interstitial fluid volume to alveolar fluid clearance in mice: ventilated vs. in situ studies. *J Appl Physiol* **89**, 672–679.

Hughey RP, Bruns JB, Kinlough CL & Kleyman TR (2004). Distinct pools of epithelial sodium channels are expressed at the plasma membrane. *J Biol Chem* **279**, 48491–48494.

Hummler E, Barker P, Gatzy J, Beermann F, Verdumo C, Schmidt A, Boucher RC & Rossier BC (1996). Early death due to defective neonatal lung liquid clearance in alpha-ENaC-deficient mice. *Nat Genet* **12**, 325–328.

Hummler E, Barker P, Talbot C, Wang Q, Verdumo C, Grubb B, Gatzy J, Burnier M, Horisberger J-D, Beermann F, Boucher R & Rossier BC (1997). A mouse model for the renal salt–wasting syndrome pseudohypoaldosteronism. *Proc Natl Acad Sci U S A* **94**, 11710–11175.

Jain L, Chen XJ, Ramosevac S, Brown LA & Eaton DC (2001). Expression of highly selective sodium channels in alveolar type II cells is determined by culture conditions. *Am J Physiol Lung Cell Mol Physiol* **280**, L646–L658.

Jiang X, Ingbar DH & O'Grady SM (1998). Adrenergic stimulation of $Na^+$ transport across alveolar epithelial cells involves activation of apical $Cl^-$ channels. *Am J Physiol Cell Physiol* **275**, C1610–C1620.

Jiang X, Ingbar DH & O'Grady SM (2001). Adrenergic regulation of ion transport across adult alveolar epithelial cells: effects on $Cl^-$ channel activation and transport function in cultures with an apical air interface. *J Membr Biol* **181**, 195–204.

Johnson MD, Bao H-F, Helms MN, Chen X-J, Tigue Z, Jain L, Dobbs LG & Eaton DC (2006). Functional ion channels in pulmonary alveolar type I cells support a role for type I cells in lung ion transport. *Proc Natl Acad Sci U S A* **103**, 4964–4969.

Johnson MD, Widdicombe JH, Allen L, Barbry P & Dobbs LG (2002). Alveolar epithelial type I cells contain transport proteins and transport sodium, supporting an active role for type I cells in regulation of lung liquid homeostasis. *Proc Natl Acad Sci U S A* **99**, 1966–1971.

Kaner RJ, Ladetto JV, Singh R, Fukuda N, Matthay MA & Crystal RC (2000). Lung overexpression of the vascular endothelial growth factor gene induces pulmonary oedema. *Am J Respir Cell Mol Biol* **22**, 657–664.

Li T & Folkesson HG (2006). RNA interference for $\alpha$-ENaC inhibits rat lung fluid absorption in vivo. *Am J Physiol Lung Cell Mol Physiol* **290**, L649–L660.

Liddle GW, Bledsoe T & Coppage WS (1963). A familial renal disorder simulating primary aldosteronism but with negligible aldosterone secretion. *Trans Assoc Am Physicians* **76**, 199–213.

Mall M, Button B, Schubert S, Pradervand S, Hummler E, Rossier BC, Grubb BR & Boucher RC (2006). Relationship between CFTR expression, airway $Na^+$ transport, ASL volume and lung disease in ENaC mouse models. *Proc Am Thorac Soc* **3**, A784.

Matalon S & O'Brodovich H (1999). Sodium channels in alveolar epithelial cells: molecular characterization, biophysical properties, and physiological significance. *Annu Rev Physiol* **61**, 627–661.

Matthay MA, Folkesson HG & Clerici C (2002). Lung epithelial fluid transport and the resolution of pulmonary oedema. *Physiol Rev* **82**, 569–600.

Matthay MA, Landolt CC & Staub NC (1982). Differential liquid and protein clearance from the alveoli of anesthetized sheep. *J Appl Physiol* **53**, 96–104.

Matthay MA & Wiener-Kronish JP (1990). Intact epithelium barrier function is critical for the resolution of alveolar oedema in humans. *Am Rev Respir Dis* **142**, 1250–1257.

Muanprasat C, Sonawane ND, Salinas D, Taddei A, Galietta LJV & Verkman AS (2004). Discovery of glycine hydrazide pore-occluding CFTR inhibitors: mechanism, structure-activity analysis, and in vivo efficacy. *J Gen Physiol* **124**, 125–137.

Parlakian A, Charvet C, Escoubet B, Mericskay M, Molkentin JD, Gary-Bobo G, De Windt LJ, Ludovsky M-A, Paulin D, Daegelen D, Tuil D & Li Z (2005). Temporally controlled onset of dilated cardiomyopathy through disruption of the *SRF* gene in adult heart. *Circulation* **112**, 2930–2939.

Pittet JF, Wiener-Kronish JP, McElroy MC, Folkesson HG & Matthay MA (1994). Stimulation of lung epithelial liquid clearance by endogenous release of catecholamines in septic shock in anesthetized rats. *J Clin Invest* **94**, 663–671.

Planès C, Blot-Chabaud M, Matthay MA, Couette S, Uchida T & Clerici C (2002). Hypoxia and $\beta_2$-agonists regulate cell surface expression of the epithelial sodium channel in native alveolar epithelial cells. *J Biol Chem* **277**, 47318–47324.

Planès C, Escoubet B, Blot Chabaud M, Friedlander G, Farman N & Clerici C (1997). Hypoxia downregulates expression and activity of epithelium sodium channels in rat alveolar epithelial cells. *Am J Respir Cell Mol Biol* **17**, 508–518.

Planès C, Leyvraz C, Uchida T, Angelova MA, Vuagniaux G, Hummler E, Matthay MA, Clerici C & Rossier BC (2005). In vitro and in vivo regulation of transepithelial lung alveolar sodium transport by serine proteases. *Am J Physiol Lung Cell Mol Physiol* **288**, L1099–L1109.

Pradervand S, Barker PM, Wang Q, Ernst SA, Beermann F, Grubb BR, Burnier M, Schmidt A, Bindels RJM, Gatzy JT, Rossier BC & Hummler E (1999*a*). Salt restriction induces pseudohypoaldosteronism type 1 in mice expressing low levels of the $\beta$-subunit of the amiloride-sensitive epithelial sodium channel. *Proc Natl Acad Sci U S A* **96**, 1732–1737.

Pradervand S, Vandewalle A, Bens M, Gautschi I, Loffing J, Hummler E, Schild L & Rossier BC (2003). Dysfunction of the epithelial sodium channel expressed in the kidney of a mouse model for Liddle syndrome. *J Am Soc Nephrol* **14**, 2219–2228.

Pradervand S, Wang Q, Burnier M, Beermann F, Horisberger J-D, Hummler E & Rossier BC (1999*b*). A mouse model for Liddle's syndrome. *J Am Soc Nephrol* **10**, 2527–2533.

Ridge KM, Olivera WG, Salsias F, Azzam Z, Hirowitz S, Rutschman DH, Dumasius V, Factor P & Sznajder JI (2003). Alveolar type 1 cells express the $\alpha$2 Na,K-ATPase, which contributes to lung liquid clearance. *Circ Res* **92**, 453–460.

Schild L, Canessa CM, Shimkets RA, Gautsghi I, Lifton RP & Rossier BC (1995). A mutation in the epithelial sodium channel causing Liddle disease increases channel activity in the *Xenopus laevis* oocyte expression system. *Proc Natl Acad Sci U S A* **92**, 5699–5703.

Schild L, Lu Y, Gautschi I, Schneeberger E, Lifton RP & Rossier BC (1996). Identification of a PY motif in the epithelial Na channel subunits as a target sequence for mutations causing channel activation found in Liddle syndrome. *EMBO J* **15**, 2381–2387.

Shimkets RA, Warnock DG, Bositis CM, Nelson-Williams C, Hansson JH, Schambelan M, Gill JR Jr, Ulrik S, Milora RV, Findling JW, Canessa CM, Rossier BC & Lifton RP (1994). Liddles's syndrome: heritable human hypertension caused by mutations of the $\beta$ subunit of the epithelial sodium channel. *Cell* **79**, 407–414.

Snyder PM (2000). Liddle's syndrome mutations disrupt cAMP-mediated translocation of the epithelial $Na^+$ channel to the cell surface. *J Clin Invest* **105**, 45–53.

Verghese GM, Ware LB, Matthay BA & Matthay MA (1999). Alveolar epithelial fluid transport and the resolution of clinically severe hydrostatic pulmonay oedema. *J Appl Physiol* **87**, 1301–1312.

Ware LB & Matthay MA (2001). Alveolar fluid clearance is impaired in the majority of patients with acute lung injury and the acute respiratory distress syndrome. *Am J Respir Crit Care Med* **163**, 1376–1383.

## Acknowledgements

We would like to thank Dr Michael Matthay, Dr Xiaohui Fang, Dr Paul Soler, Dr Alain Vandewalle and Dr Evelyne Ferrary for helpful suggestions, Sylviane Couette and Céline Leyvraz for technical assistance, and Olivier Thibaudeau (CEFI IFR02, Faculté de Médecine Bichat, Université Denis Diderot-Paris7) for his help with the histology. This work was supported by INSERM, by Fondation du Legs Poix, and by the Swiss National Foundation (Grant FNRS no. 3100AO-102125/1 to E. Hummler and B. C. Rossier).